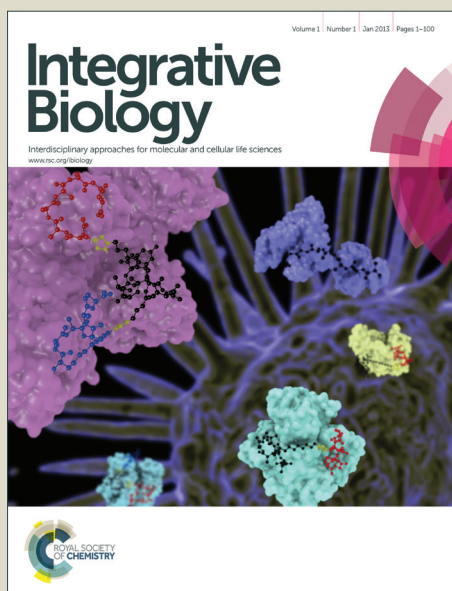


Integrative Biology

Accepted Manuscript



This is an *Accepted Manuscript*, which has been through the Royal Society of Chemistry peer review process and has been accepted for publication.

Accepted Manuscripts are published online shortly after acceptance, before technical editing, formatting and proof reading. Using this free service, authors can make their results available to the community, in citable form, before we publish the edited article. We will replace this *Accepted Manuscript* with the edited and formatted *Advance Article* as soon as it is available.

You can find more information about *Accepted Manuscripts* in the [Information for Authors](#).

Please note that technical editing may introduce minor changes to the text and/or graphics, which may alter content. The journal's standard [Terms & Conditions](#) and the [Ethical guidelines](#) still apply. In no event shall the Royal Society of Chemistry be held responsible for any errors or omissions in this *Accepted Manuscript* or any consequences arising from the use of any information it contains.

Insight Box Statement

- **Insight:** We obtained new data on the mechanisms of motility and polarization of T cell interacting with the target cell. We demonstrated that the motility and polarity of T cell *in vitro* can be mediated by differential adhesion through the long, flexible microtubule-containing appendages, and we speculated that this mechanism may take place *in vivo*.
- **Innovation:** We combined an established experimental biomimetic model of T cell polarization, treatment with cytoskeleton-targeted drugs, high-resolution live-cell confocal and transmitted-light imaging, and image processing and analysis of multidimensional images of individual cells.
- **Integration:** We demonstrate that integrating advanced imaging, experimental modeling, biophysics and cell biology is extremely helpful for studying the mechanisms of immunodeficiency at sub-cellular level.

Cite this: DOI: 10.1039/c0xx00000x

www.rsc.org/xxxxxx

ARTICLE TYPE

Microtubule Appendages Mediating T-Cell Motility and Polarity

Sergey N. Arkhipov^{*a,b} and Ivan V. Maly^{b,c}

Received (in XXX, XXX) Xth XXXXXXXXX 20XX, Accepted Xth XXXXXXXXX 20XX

DOI: 10.1039/b000000x

5 Polarization of the centrosome and Golgi apparatus in the T cell (TC) toward the antigen-presenting cell (APC) is essential for the specificity of the immune response on the cellular level. Previously we reported existence of thin, long processes on the TC surface, which emanated predominantly from the area next to the Golgi apparatus. They appeared to be involved in the orientation of the TC during the initial phases of its attachment, which preceded the formation of the immunological synapse mediated by lamellipodia. 10 Here we improve visualization of the long, thin protrusions in cultured TC and demonstrate using cytoskeleton inhibitors and immunofluorescence that microtubules form their cytoskeletal basis. The protrusions are seen prior to the attachment and the development of the broad lamellipodia (within a few minutes). We propose the term “tubulopodia” for this distinct type of cell appendages. Using an established experimental model that replaces the APC surface with a biomimetic substrate coated with 15 antibodies against the TC receptor (TCR), we demonstrate that abrogation of the lamellipodia-mediated synapse formation does not impede orientation of the TC Golgi apparatus and the centrosome to the contact area. Videomicroscopy reveals spreading of the tubulopodia on the TCR-binding substrate, which results in the area of their emanation, and consequently the Golgi apparatus and the centrosome, being closely apposed (polarized) to the TCR-binding surface. Treatment with paclitaxel made the tubulopodia 20 rigid, preventing their attachment to the TCR-binding surface and the reorientation of the cell body with the intracellular structures. We speculate that the motility and polarity of TC *in vivo* may be mediated in large measure by differential adhesion through the long, flexible tubulopodia.

Introduction

25 T cells (TC) conjugate with antigen-presenting cells (APC) and secrete mediators of the immune response, the nature of which (regulatory or cytotoxic) depends on the nature of the antigen and the cell that presents it. In either case, the formation of the close contact, and the directionality of the secretion are believed to be 30 crucial for achieving immunological specificity in the context of the dense tissue, where the TC-APC conjugate is surrounded by bystander cells¹. Orientation of the centrosome and Golgi apparatus in the TC to the area of contact with the APC are the structural correlates of this directionality²⁻³. A widely used 35 experimental model for studying the conjugation of TC with APC and the orientation of the secretory apparatus in the TC consists in presenting Jurkat T lymphocytes, which are cultured in suspension, with a substrate coated with antibodies against the T-cell receptor (TCR, CD3)⁴⁻⁵. Formation of a broad contact 40 between the body of a Jurkat cell and the biomimetic substrate, and orientation of the centrosome, around which the secretory Golgi apparatus in T lymphocytes is assembled, to this substrate, have long been described⁴⁻⁷.

Recently we described long processes emanating from the 45 surface of the Jurkat T lymphocytes⁸. Attachment of these processes to the biomimetic substrate was followed by their

disappearance, presumed to be retraction. It preceded the lamellipodia mediated development of the broad contact area between the cell body and the substrate. On the basis of our 50 experiments, we proposed that the conjugation was initiated by the long surface processes. Since these processes emanated predominantly from the area on the cell surface under which the Golgi apparatus was located, attachment of their free ends and subsequent retraction appeared to drive the reorientation of the 55 cell body in such a direction as to bring the Golgi apparatus closer to the substrate. We proposed that the long surface processes not only initiated the contact, but their retraction also contributed to the establishment of the functional orientation of the TC⁸.

60 In the present work, we improved visualization of these processes, addressed the question of their cytoskeletal basis, and probed experimentally the cell motility that they mediate. The new results establish that these surface processes are a class of appendages that are unique in their structure and function, 65 justifying introduction of a new term, “tubulopodia”.

Materials and methods

Jurkat cells were grown and prepared for observation essentially as described before^{5,8}. The cells were grown in complete culture media RPMI 1640 with 25 mM HEPES (Mediatech, Herdon,

VA), 10% fetal bovine serum (Lonza, Wakersville, MD), 100 U/ml penicillin, and 100 U/ml streptomycin (Biosource, Rockville, MD). The cell suspension was concentrated by centrifugation at 1000 rpm for 2 minutes, and injected into the observation chamber (LabTek, Nunc, Rochester, NY). The glass bottom of the chamber was pre-coated with poly-L-lysine (Sigma) and with antibodies against CD3 (clone UCHT1, Pharmingen, San Diego, CA).

Cytoskeletal inhibitors were obtained from Sigma (St. Louis, MO). The concentrations and incubation times were 10 μ M and 1 h for cytochalasin D, 10 μ M and 30 min for nocodazole, and 1 μ M and 1 h for paclitaxel.

For live-cell fluorescence microscopy, the following staining procedures were used. To visualize the cell surface and the Golgi apparatus, the cell membranes were labelled prior to the observation with 5 μ M BODIPY TR C5-ceramide (Invitrogen, Carlsbad, CA) combined with bovine serum albumin (Fisher, Fair Lawn, NJ) according to the manufacturer's instructions for 45 min. To visualize the centrosome, the microtubules were labeled prior to observation with 100 nM Oregon Green Tubulin Tracker (Invitrogen) for 30 min.

Uniform conditions were ensured in the different experiments.

Where the experiment involved treating the cells in more than one way, the treatments were concurrent. Where the duration of incubation with the different reagents was not identical, the last part of the longer incubation ran concurrently with the shorter one. DMSO (Acros Organics, Geel, Belgium) was used as the solvent for the cytoskeletal inhibitors. Its final concentration in the culture medium was 1% (by volume) in all experiments, and the cells not treated with any inhibitors were exposed to the solvent identically. The vital staining reagents were not present in the medium used after the centrifugation step and during the observation, but the cytoskeletal inhibitors and DMSO were. Cells were maintained at 37 °C and 5% CO₂ in the tissue culture incubator, and at 37 °C on the microscope stage, using an ASI 400 air stream incubator (Nevtek, Burnsville, VA).

Transmitted-light phase-contrast and fluorescence images were acquired with a Nikon TE 200 inverted microscope (Nikon, Melville, NY). The 60 \times planapochromatic water-immersion objective with numerical aperture 1.2 (Nikon) was actuated by a PIFOC 721 piezo-positioner (Physik Instrumente, Auburn, MA). Fluorescence images were acquired using a CARV II spinning-disc attachment (BD, Franklin Lakes, NJ), and a light source X-cite (EXFO, Mississauga, Ontario). ORCA II ERG camera was used (Hamamatsu Photonics, Bridgewater, NJ). The imaging hardware was controlled by IPLab software (Scanalytics, Rockville, MD), which was also used for image analysis. The voxel size in three-dimensional images was 0.22 μ m horizontally and 0.4 μ m vertically. Each three-dimensional image was acquired over 7.5 s. Additionally, two-dimensional transmitted-light phase-contrast images were acquired with the time resolution 1 s and pixel size 0.11 μ m.

The modifications of the above live-cell protocol for immunofluorescence staining were the following. Poly-L-lysine-coated cover glasses (BD) were used instead of the LabTek chambers, and within 5 min of exposure to the anti-CD3-coated substrate, the cells were fixed and permeabilized for 30 minutes at room temperature in phosphate buffer solution (Fisher)

containing 0.15% glutaraldehyde (Acros), 0.1% Triton X100 (Sigma), 10 mM EGTA (Boston Bioproducts, Boston, MA), and 10 mM MgCl₂ (Teknova, Hollister, CA). Subsequent to blocking with 0.1% sodium borohydride (Acros), the specimen was stained with mouse anti- α -tubulin antibodies (Sigma) and Alexa 488 or TRITC-conjugated goat anti-mouse antibodies (Invitrogen).

The specimens were embedded in Antifade medium (Invitrogen) and imaged with a 100 \times planapochromatic objective (numerical aperture 1.4) with the voxel size 0.065 μ m horizontally and 0.4 μ m vertically.

Where indicated, different treatment of the chamber bottom was used for studies of the cell morphology: it was coated with 10 μ g/ml human plasma-derived fibronectin (R&D Systems, Minneapolis, MN) overnight at 4 °C, blocked with 2% bovine serum albumin, and washed with phosphate buffer solution (Fisher Scientific, USA).

The cells were scored for the polarization by examining the three-dimensional confocal images. The cells were considered polarized if they display the centroid of fluorescently stained Golgi apparatus within the bottom 2 μ m of the cell, i.e. within 2 μ m from stimulatory substrate.

Results

When the suspension of Jurkat TC is presented with the substrate coated with stimulatory antibodies against the TCR, these normally non-adherent cells attach to the substrate, develop broad circular lamellipodia, and orient their centrosome and Golgi apparatus to the substrate (Fig. 1, 2). In addition to these well-known effects, as reviewed above, we observe the existence of finger-like protrusions on the cell surface, often in bunches and next to the intrinsically asymmetrical Golgi apparatus. These are seen prior to the attachment (within a few minutes), but not following the development of the broad lamellipodia (Fig. 1).

New computer-enhanced images (Fig. 3) and high-resolution images of cells loaded with a fluorescent membrane probe (Fig. 4) revealed the full extent of these unusual surface processes. Their emanation predominantly from the area next to the centrosome and Golgi apparatus (these two organelles are colocalized asymmetrically in the nearly spherical cell body, Fig. 2B) was suggestive of their being linked to the asymmetric microtubule cytoskeleton.

Immunofluorescence imaging (Fig. 5) showed microtubules that appeared to separate from the cell body. The difficulty of correlating such microtubules in the immunofluorescence images with the much more extended surface processes in the live-cell images (Fig. 3, 4) could be attributed to the effects of fixation. It could also be attributed to loss of the less firmly attached cells from the fixed specimens, taken together with the fact that the narrow processes were disappearing during the development of the broad lamellipodia (Fig. 1). Nonetheless, the unusual extent (Fig. 3, 4) and apparent connection to the microtubule cytoskeleton (Fig. 5) indicated that these processes were of a novel type, and suggested the new term "tubulopodia" to denote them. According to analysis of the immunofluorescence images, each tubulopodium of untreated cells consist of one or more microtubules. Microtubules extend all the way to the termini of tubulopodia.

The quantitative contribution of tubulopodia into the TC

reorientation was difficult to assess in the experiments described above. A number of cells reoriented in large part, or mostly, before the onset of lamellipodia-mediated spreading, as illustrated in Fig. 1C-N. However, the asynchrony of these events in individual cells, and the eventual polarization and spreading of nearly all of them precluded reliable measurement of the relative contribution of the part of the reorientation that occurred prior to the spreading. To study the motility mediated by tubulopodia in its pure form, and to assess quantitatively its capacity to orient the TC body, we inhibited lamellipodia formation with cytochalasin D. This treatment did not significantly affect the capacity of cells for reorientation (Fig. 2C), despite the complete abrogation of lamellipodia-mediated spreading (Fig. 6). This outcome was in agreement with experiments in which the lamellipodial spreading was inhibited by interfering with Apr2/3 activation⁹. Since tubulopodia were not suppressed in our experiment with cytochalasin (Fig. 6), this experiment suggested that the reorientation function was attributable to tubulopodia.

In fact, the treatment with cytochalasin D enhanced the prominence of tubulopodia (Fig. 7AB). This made possible better visualization of MTs in them (Fig. 8). It also helped reveal an unequivocal suppression of the tubulopodial morphology by nocodazole. Application of nocodazole alone, without cytochalasin, led primarily to gross deformation of the cells (Fig. 7C). The resulting morphology was difficult to interpret with regard to the question of tubulopodia suppression by the drug. In contrast, addition of nocodazole to cytochalasin diminished the tubulopodia unequivocally compared to the cells treated with cytochalasin alone (compare Fig. 7 panels D and B). As might be expected based on these results, combined treatment with cytochalasin and paclitaxel produced the most robust tubulopodia (Fig. 7F, Fig. 9). Together, these results point to the importance of the microtubule cytoskeleton for the tubulopodial morphology, and to unimportance, and even moderating action, of the actin cytoskeleton.

The addition of nocodazole to cytochalasin inhibited the T-cell body orientation (Fig. 2C). Although this effect could be attributed to the suppression of tubulopodia by the nocodazole, it could also be explained by the well-known general requirement of the microtubule cytoskeleton (in the cell body) for the polarization of the centrosome and Golgi apparatus in T cells¹. The inhibition of the polarization by nocodazole alone was reproduced also in this series of experiments (Fig. 2C). The inhibition of the orientation by addition of paclitaxel to cytochalasin (Fig. 2C) was in comparison informative, because neither cytochalasin alone nor paclitaxel alone inhibited orientation (Fig. 2C). The absence of the effect of paclitaxel alone on polarization was in agreement with the previous work^{10 11}. While microtubules in tubulopodia of the drug-treated TC may experience various dynamics (e.g. a taxol-induced increase in the length of the microtubules), our previous experimental and computational data indicated that microtubule dynamics are not essential for the TC polarization¹¹. We did not find any significant dynamics on a short time scale (e.g. growth, shrinkage) in tubulopodia of the untreated TC.

To determine the novel mechanism of polarization that was uniquely sensitive to paclitaxel, more detailed dynamic observations were conducted. Time-lapse recording (Fig. 10)

revealed that the bunched tubulopodia adhered to (flattened on) the substrate. This was accompanied by, and presumably caused, translation and rotation of the cell body. The initial state most commonly was a cell with a bunch of tubulopodia emanating to the side of the cell, and unattached to the substrate. The final state most commonly was one in which the area of the tubulopodia emanation on the cell surface was in immediate opposition to the substrate, and the cell body was on top of the splayed-out bunch of the tubulopodia on the substrate. This observation from the image sequences in Fig. 1 and 6 is consistent with the higher-time-resolution sequences in Fig. 10. The flexibility of the tubulopodia appeared to permit their adhesion to the substrate and the splaying of the bunch on the time-scale of seconds. The adhesion of tubulopodia to the substrate can be accompanied by their significant bending which depends on their rigidity (Fig. 11C). The adhesion, in turn, appeared to drive the movement of the cell body. The orientation of the area of emanation of the tubulopodia to the substrate can be discerned in the later images from the timelapse sequences as the appearance of the “dotted” refractive pattern in the optical section next to the substrate, which section was imaged (Fig. 10). The attachment of tubulopodia to the substrate can be discerned as their gradually coming into focus in the same optical section near the substrate. The movements and deformations discernible in the time-lapse observations were consistent also with the immunofluorescence data, which were presented above and which can be interpreted as three-dimensional snapshots of the different stages of tubulopodia adhesion and cell body reorientation, due to the significant asynchrony of individual cells in the experiment.

In the light of these dynamics of cells untreated with paclitaxel, we hypothesized that the effect of paclitaxel could be due to its increasing the rigidity of the tubulopodia, and thus turning them from active appendages into an obstacle for cell-body reorientation. Indeed, the “robust” tubulopodia of paclitaxel-treated cells appeared (Fig. 7F, 9) too rigid to support the above motility mechanism. Their consistent optical thickness and straightness in these images suggested that they might be incapable of bending sufficiently to accommodate their own attachment to the substrate and the movement of the cell body into its normal final orientation. Measurements confirmed that tubulopodia in cells treated with paclitaxel in addition to cytochalasin were less flexible than those in cells treated with cytochalasin alone (Fig. 11).

The ratio of the end-to-end distance to the contour length of tubulopodia was significantly higher (i.e. the tubulopodia were straighter) in cells treated with cytochalasin and paclitaxel than in cells treated with cytochalasin alone. In addition, this ratio did not change significantly with time in cells treated with both drugs, whereas it significantly decreased (indicating tubulopodia bending) in cells treated with cytochalasin alone (on the level of $p=0.05$ in the Mann-Whitney test, see Fig. 11C). These dynamic observations and measurements were consistent with the immunofluorescence images of the paclitaxel-treated cells (Fig. 9), where the microtubule bundles forming the basis of the “robust” tubulopodia were not often seen bending along the substrate. Although the immunofluorescence data suggested bundling (Fig. 9), paclitaxel had also been reported to increase rigidity of individual microtubules *in vitro*¹², which would also be

consistent with our rigidity measurements done on tubulopodia of paclitaxel-treated living cells (Fig. 11).

Discussion

Our new visualization efforts demonstrate a greater extent and number of the narrow processes on the surface of Jurkat T lymphocytes than was reported before⁸. The role of microtubules as the cytoskeletal basis of these protrusions is demonstrated by the effect of cytoskeletal inhibitors as well as by immunofluorescence data. Cytochalasin D only enhanced the prominence of these processes, indicating that the actin component was not essential, and that this component perhaps had a moderating rather than promoting influence on their morphogenesis. Their suppression by nocodazole and their enhancement by taxol (when these drugs were added to cytochalasin) also indicated that the microtubule component was the crucial one. This sets the processes described here apart from filopodia, microvilli, or nanotubes, which have been described on the surfaces of lymphocytes before^{13 14 15}. At the same time, the microtubular basis of the processes we describe here places them in the same category as the protrusions that were shown to enhance attachment of malignant cells of epithelial origin¹⁶. The latter protrusions were similarly promoted by the addition of cytochalasin. In our study we did not score tubulopodia of lymphocytes for enrichment in detyrosinated Glu-tubulin as in the study¹⁶, however a presence of this post-translationally modified form of α -tubulin in the TC tubulopodia could be also suggested. Isolated narrow protrusions containing microtubules were also seen on axon shafts¹⁷, although their relation to the ones we are describing here, and their function, are less clear. Further, the appendages described here are clearly different from cilia. Microtubules in each of the protrusions seen in our images appear to run from their bases to the single centrosome in the T cell. In addition, when the microtubules in the cell body adopt the bundled appearance following treatment with paclitaxel, the same changes occur in the ones that enter the appendages (Fig. 9). Neither of these observations should be compatible with the microtubule cytoskeleton structure characteristic of cilia. It must be mentioned that microtubules are known to be associated with filopodia in neuronal growth cones. In precise terms, however, these microtubules rarely enter the growth cone filopodia as such, associating instead with what is known as filopodial actin bundles or microspikes, which are the intralamellipodial "roots" of the filopodial cytoskeleton¹⁸.

The above distinctions justify the term "tubulopodia", which reflects the peculiar cytoskeletal basis (microtubules) of the appendages characterized in this work. Generalizing the attachment function of these appendages as described for T cells here, and the attachment function described in the referenced experiments on malignant epithelial cells, we propose that the characteristic function of tubulopodia is attachment. Due to the considerable length and polar arrangement of the tubulopodia, the attachment that they mediate can cause significant movement and reorientation of the cell body, as discussed below.

The ability of tubulopodia to polarize (orient) the body of the cell is demonstrated by video observations following decoupling the polarization from cell spreading with cytochalasin. In the experimental model used here, as well as in the models that

involve interaction of TC with other cells in culture, the spreading of the TC is rapidly induced when the TC body comes in contact with the target surface, be it the other cell or the TCR-binding substrate. The onset of spreading appears to preclude any subsequent action of the narrow processes, as well as promote their disappearance due to the relative conservation of the cell surface area⁸. At the same time, spreading sets the stage for the action of the compactization forces in the cell body, which respond to the flattening deformation^{11 19 20}. As was analyzed in the cited articles, the elastic compactization forces and the molecular-motor forces can cause reorientation of the centrosome and Golgi apparatus to the interface with the target, once this interface is formed by spreading. Exploiting the variability of timing among individual TC, we were able to show previously that at least in some of them, part of the reorientation of the cell body with respect to the target surface precedes the spreading, and can therefore be attributed to the action of the narrow processes that we now call tubulopodia⁸.

Nonetheless, even in those cases the onset of spreading is accompanied by disappearance of the narrow processes, presumably by retraction due to the conservation of the cell surface area. This led to the mechanical model in which it is the process retraction that was driving the cell body reorientation⁸. The new experiments show that when spreading is fully suppressed by cytochalasin, the narrow processes (tubulopodia) do not retract, yet the cell body reorientation that is achieved is quite complete. The absence of rapid spreading permitted detailed video observations. The video data show that attachment to the substrate of the tubulopodia, which emanate predominantly from that pole of the cell body where the centrosome and Golgi apparatus are located, brings that pole of the cell body to the substrate when the tubulopodia become maximally attached. These video observations (Fig. 10) are consistent with the appearance of the microtubule cytoskeleton in the cell body and in the processes in immunofluorescence images (Fig. 5, 8). In the light of the video data showing the progressive movement and rotation of the cell body in the direction of the progressively flattening bunch of the surface processes, those of the immunofluorescence images in which more processes are seen unattached to the substrate can be interpreted as cells fixed early in their reorientation, given the individual cells' asynchrony. In the same light, other cells can be seen as having been fixed later in their individual timeframe, when the centrosome is already next to the substrate and most of the processes have fully adhered to the substrate (compare Fig. 5AD or Fig. 8AD on the one hand with Fig. 8CF on the other).

Thus, the new experiments have demonstrated a new mechanism of orientation of the interior structure of the TC with respect to the target surface: movement and rotation of the entire TC body, which is driven by receptor-mediated adhesion of the tubulopodia emanating from the centrosome-Golgi area. To improve the observation of this mechanism in vitro, the cell spreading had to be experimentally abrogated, as discussed above. The new results therefore raise the question: which of the mechanisms – the one mediated by the formation of the synapse by spreading, or the one mediated by the tubulopodia adhesion – should be expected to play the leading role in vivo? The tubulopodia that we describe here are below the detection limit of

today's intravital imaging techniques, and the histological data are also usually acquired at a far lower resolution than would be necessary for their detection. In addition, the thin sections usually employed in the comparatively high-resolution histology are not likely to contain sufficiently long segments of sufficiently numerous tubulopodia that would permit reliable detection of them, given their three-dimensional distribution. A notable exception was the apparently thick sections of spleen examined at an uncommonly high magnification in a study on multiple sclerosis²¹, the difference in the technique presumably stemming from the study's primary focus on neurohistology. The images showed a structure of T lymphocytes in the spleen that is remarkably close to what we see in our new in-vitro images: very long, narrow, straight processes emanating in a diverging bunch from what appears to be a focal point on the rounded body of the lymphocyte. (The archival electronic version of the cited paper has insufficient resolution; refer to the original printed journal.)

Awaiting dynamic data of sufficient resolution, the following speculation is permitted. Under the conditions of all in-vitro experiments heretofore conducted, not only are the long processes difficult to visualize, but more importantly the body of the T cell easily comes in contact with the target surface (another cell, or the biomimetic substrate). This sets off spreading, synapse formation, and thus directs the polarization of the interior structures in significant measure along the biomechanical pathways that act inside the cell body and have been studied previously [e.g., ^{11 19 20}]. In contrast, under the conditions that prevail in vivo, the movement of the T lymphocyte body is restricted by the structure of the dense tissue. The contact with the target surface is therefore much more likely to be established through the long, narrow processes such as the tubulopodia. Indeed, tubulopodia would be able to penetrate the tissue and probe a significant volume of it in search of the target, for which the receptors on them would have affinity. The body of the lymphocyte would only come in direct contact with the target after a significant period of time, during which the lymphocyte body and the target would be connected via the long, narrow tubulopodium, or via several of them. One can then conjecture also that the progressive adhesion of the tubulopodia, initiated nearer to their tips, and propagating toward the point of their emanation from the lymphocyte body, similar to the dynamics seen in our in-vitro videos, would be the mechanism through which the lymphocyte body could reach the target in the tissue. Importantly, like in our in-vitro experiments, the establishment of contact by the microtubule-based tubulopodia emanating from the centrosome area, and propagation of adhesion toward their bases, would bring the lymphocyte body in direct contact with the target already in the immunologically functional orientation, with the secretory (Golgi) apparatus facing the target (Fig. 12).

In the framework set by our hypothesis, it will be important to study the question of how the tubulopodia could penetrate the tissue, and thus the question of their origin in general, which was not addressed in the present work. Tubulopodia may be generated through assembly of microtubules away from the cell body, or alternatively through lateral separation of a microtubule, or a microtubule bundle, from the cortical "basket" of microtubules that is characteristic of lymphocytes. Dedicated studies will also be necessary to establish whether the force of the tubulopodia

adhesion in the structural context of the tissue could be sufficient to drive the movement of the lymphocyte body to the target. Our measurements demonstrate the importance of flexibility of the tubulopodia for their function: increasing their rigidity by bundling the microtubules with paclitaxel apparently creates a mechanical impediment to the movement of the cell body that the adhesion force cannot overcome even in vitro. The in-vivo motility and polarization mechanism that is hypothesized here should therefore be possible to inhibit with paclitaxel for the purposes of therapeutic immunomodulation.

Conclusions

The experimental results presented here support a new model for T lymphocyte motility and polarization: translational movement and directed reorientation of the cell body that are driven by adhesion of long, narrow, polarized microtubule-based processes. This type of cell appendages is characterized in this paper, and the term "tubulopodia" is proposed to reflect their distinction from other types of narrow cell appendages, such as filopodia, microvilli, nanotubes, or cilia. Whereas the role that the tubulopodia-mediated motility can play in vivo remains a topic for future work, the in-vitro data presented here demonstrate that T lymphocytes are capable of such motility.

Acknowledgements

This work was supported by grant GM078332 from the National Institutes of Health (USA) and the Russian Government Program of Competitive Growth of Kazan Federal University (Russia).

Notes

* Corresponding author.

^a Institute of Fundamental Medicine and Biology, Kazan (Volga region) Federal University, Kazan, Russia. Fax: +784 3233 7814, Tel: +791 7858 3529; E-mail: sergarkh@gmail.com

^b Former Address: Department of Computational and Systems Biology, School of Medicine, University of Pittsburgh, Pittsburgh, PA 15260, USA. Fax: 41 2648 3163; Tel: 41 2648 3333

^c Present Address: Department of Physiology and Biophysics, School of Medicine and Biomedical Sciences, State University of New York, Buffalo NY, USA

References

- 1 A. Kupfer and S.J. Singer, *Annu Rev Immunol*, 1989, **7**, 309–337;
- 2 S.N. Bykovskaja, A.N. Rytenko, M.O. Rauschenbach and A.F. Bykovsky, *Cell Immunol*, 1978, **40**, 164–174;
- 3 B. Geiger, D. Rosen and G. Berke, *J Cell Biol*, 1982, **95**, 137–143;
- 4 M.V. Parsey and G.K. Lewis, *J Immunol*, 1993, **151**, 1881–1893;
- 5 S.C. Bunnell, V.A. Barr, C.L. Fuller and L.E. Samelson, *Sci STKE*, 2003, **177**, pl8;
- 6 S.C. Bunnell, V. Kapoor, R.P. Tribble, W. Zhang and L.E. Samelson, *Immunity*, 2001, **14**, 315–329;
- 7 M.R. Kuhne, J. Lin, D. Yablonski, M.N. Mollenauer, L.I.R. Ehrlich, J. Huppa, M.M. Davis and A. Weiss, *J Immunol*, 2003, **171**, 860–866;
- 8 S.N. Arkhipov and I.V. Maly, *Phys Biol*, 2008, **5**, 016006;
- 9 T.S. Gomez, K. Kumar, R.B. Medeiros, Y. Shimizu, P.J. Leibson and D.D. Billadeau, *Immunity*, 2007, **26**, 177–190;
- 10 J.D. Knox, R.E.J. Mitchel and D.L. Brown, *Cell Motil Cytoskeleton*, 1993, **24**, 129–138;

- ¹¹ A. Baratt, S.N. Arkhipov and I.V. Maly, *PLoS ONE*, 2008, **3**, e3861;
- ¹² B. Mickey and J. Howard, *J Cell Biol*, 1995, **130**, 909–917;
- ¹³ L.I. Salazar-Fontana, V. Barr, L.E. Samelson and B.E. Bierer, *J Immunol*, 2003, **171**, 2225–2232;
- ¹⁴ M.J. Brown, R. Nijhara, J.A. Hallam, M. Gignac, K.M. Yamada, S.L. Erlandsen, J. Delon, M. Kruhlak and S. Shaw, *Blood*, 2003, **102**, 3890–3899;
- ¹⁵ S. Sowinski, C. Jolly, O. Berninghausen, M.A. Purbhoo, A. Chauveau, K. Köhler, S. Oddos, P. Eissmann, F.M. Brodsky, C. Hopkins, B. Önfelt, Q. Sattentau and D.M. Davis, *Nat Cell Biol*, 2008, **10**, 211–219;
- ¹⁶ R.A. Whipple, A.M. Cheung and S.S. Martin, *Exp Cell Res*, 2007, **313**, 1326–1336;
- ¹⁷ D.J. Goldberg and D.W. Burmeister, *J Neurosci*, 1992, **12**, 4800–4807;
- ¹⁸ D.T. Burnette, A.W. Schaefer, L. Ji, G. Danuser and P. Forscher, *Nat Cell Biol*, 2007, **9**, 1360–1369;
- ¹⁹ S.N. Arkhipov and I.V. Maly, *Phys Biol*, 2006, **3**, 209–219;
- ²⁰ J.R. Kuhn and M. Poenie, *Immunity*, 2002, **16**, 111–121;
- ²¹ K. Selmaj, C.F. Brosnan and C.S. Raine, *Proc Natl Acad Sci USA*, 1991, **88**, 6452–6456.

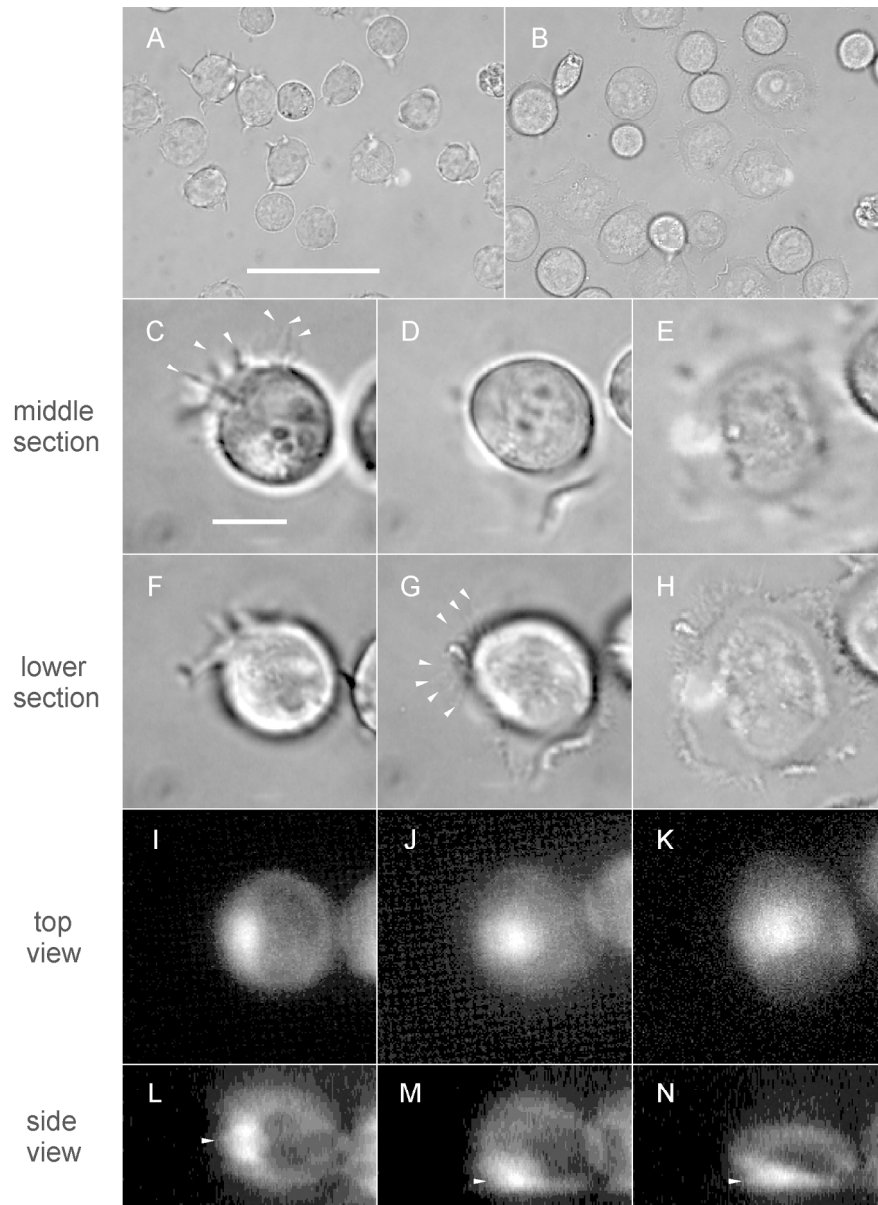


Fig. 1. Morphology, attachment, and polarization of Jurkat T lymphocytes on an anti-TCR substrate. (A) 2 min after the cell suspension was introduced into the chamber and came in contact with the substrate. Scale bar, 50 μm . (B) The same field as shown in A, 20 min after introduction of the cell suspension. (C–N) Three-dimensional time-lapse images of a representative cell. Images in the first column (C, F, I, L), in the second column (D, G, J, M), and in the third column (E, H, K, N) were taken respectively in 2, 5, and 20 min after the introduction of the cell suspension. As labeled in the figure, two optical sections imaged in transmitted light are shown, as well as the top and side views of the full three-dimensional fluorescence image. The ceramide-based fluorescent probe in I–N reveals the plasma membrane and the Golgi apparatus area. Arrowheads in C and G indicate the narrow tubulopodia. Arrowheads in L–N indicate the Golgi apparatus. The scale bar in C is 10 μm . Panels C–N refer to the same threedimensional domain and have the same scale. 156x214mm (300 x 300 DPI)

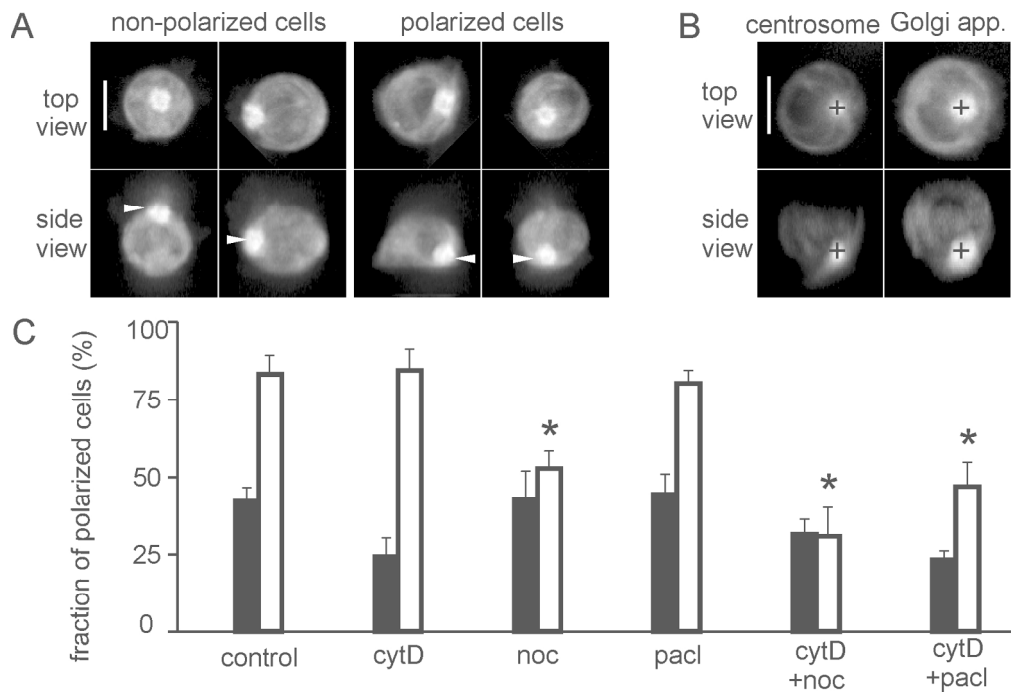


Fig. 2. Polarization of Jurkat T lymphocytes to the anti-TCR substrate. (A) Examples of cells that were categorized here as polarized and not polarized to the substrate. Two polarized and two non-polarized cells are shown, each in the top and side views on the three-dimensional image of fluorescence from a ceramide-based membrane probe. The bright Golgi apparatus area is indicated with the arrowheads. Scale bar, 10 μm . (B) Colocalization of the centrosome and Golgi apparatus in the T lymphocyte. The cell was vitally stained with tubulin tracker (showing microtubules converging on the centrosome marked with the cross) and with fluorescently labeled ceramide (showing membranes with the bright area of the Golgi apparatus marked with the cross). Scale bar, 10 μm . (C) Fraction of polarized cells 2 min (black bars) and 20 min (white bars) after bringing the cell suspension in contact with the substrate, for cells treated with the solvent only ("control"), with cytochalasin ("cytD"), nocodazole ("noc"), paclitaxel ("pacl"), with the combination of cytochalasin and nocodazole ("cytD+noc"), and with the combination of cytochalasin and paclitaxel ("cytD+pacl"). The bars and error bars show the mean and its 95% confidence interval calculated on the basis of 3 full-frame fields of view in each of the 4 independent experiments (1992 cells altogether). For the 20-min time point, the polarization levels which are significantly lower than that in the "control" group are marked with asterisks ($p < 0.05$ in the Mann-Whitney test).

164x111mm (300 x 300 DPI)

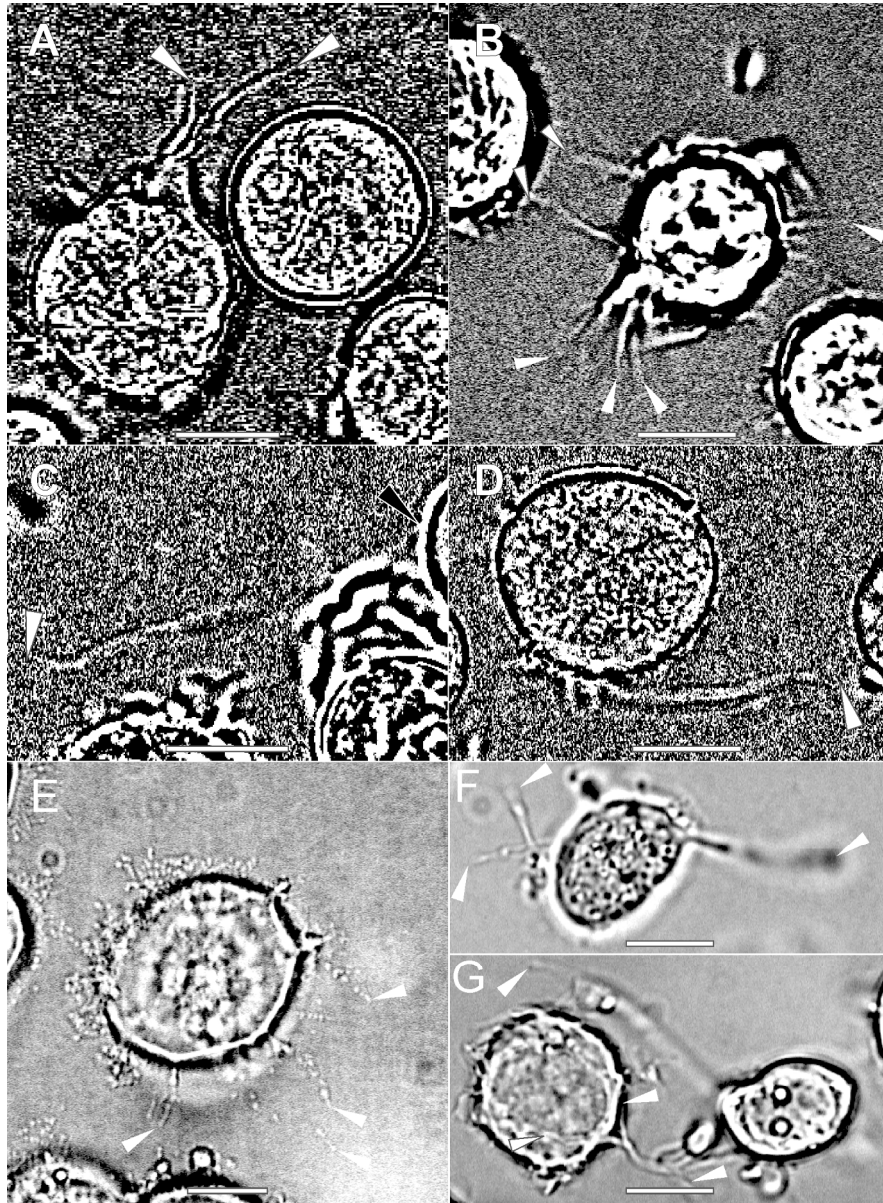


Fig. 3. Contrast-enhanced images of surface processes (tubulopodia) in living Jurkat T lymphocytes. (A, B) Contrast enhanced by subtraction of an optical section next to the substrate from an optical section farther away from the substrate. (C, D) Contrast enhanced by subtraction of frames from a time-lapse sequence.

(E, F, G) Conventional intensity scaling is sufficient to reveal some of the tubulopodia in some cells.

Arrowheads indicate tubulopodia. The cells in A and B are on glass, in C and D – on the anti-CD3-coated substrate, and in E, F, and G – on fibronectin. Scale bars, 10 μ m.

167x228mm (300 x 300 DPI)

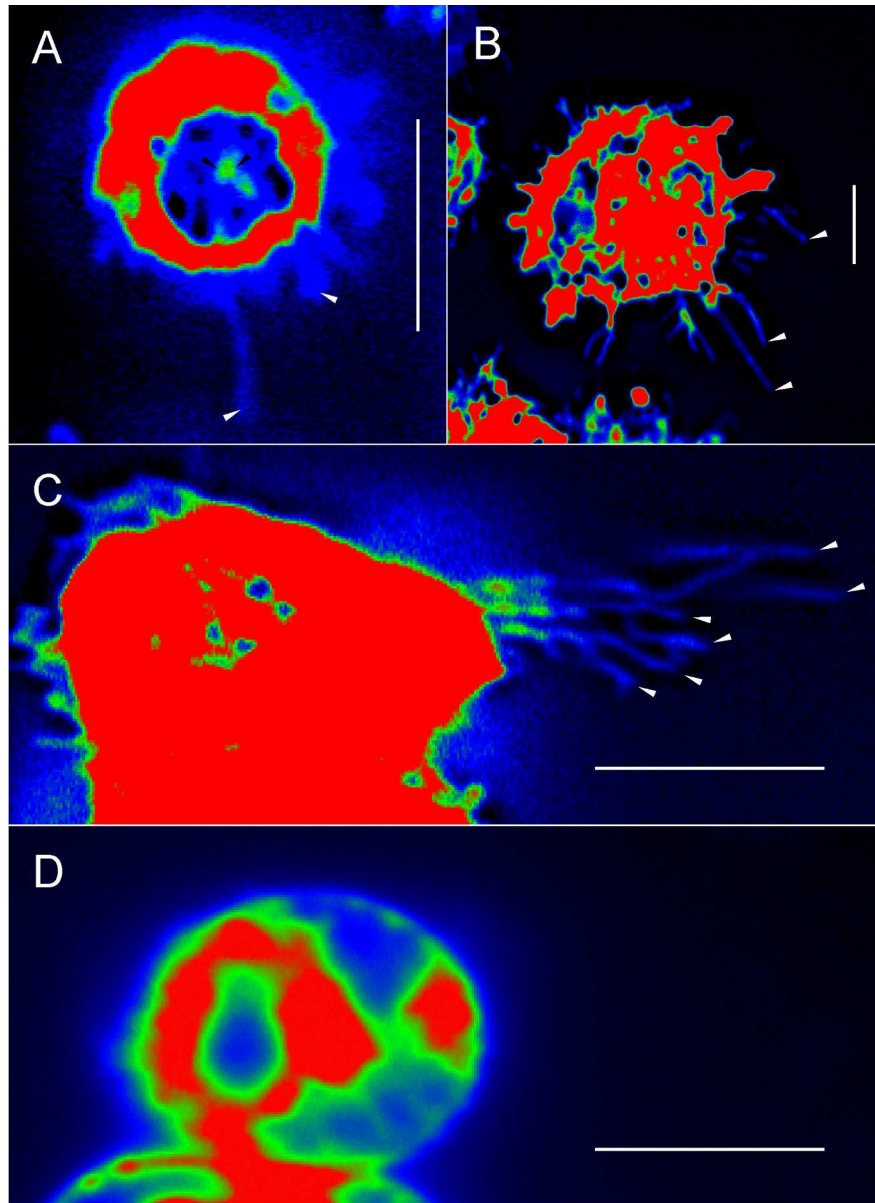


Fig. 4. Surface processes (tubulopodia) visualized in living Jurkat T lymphocytes with a ceramide-based fluorescent membrane probe. (A, B, C) Single confocal sections of three different cells. (D) A differently scaled image of the cell from panel C shows the cell body more clearly. Arrowheads indicate tubulopodia.

The pseudocolor scale is from black (lowest fluorescence intensity) to blue to green to red (highest fluorescence intensity). The cells are on fibronectin. Scale bars, 10 μm.

166x228mm (300 x 300 DPI)

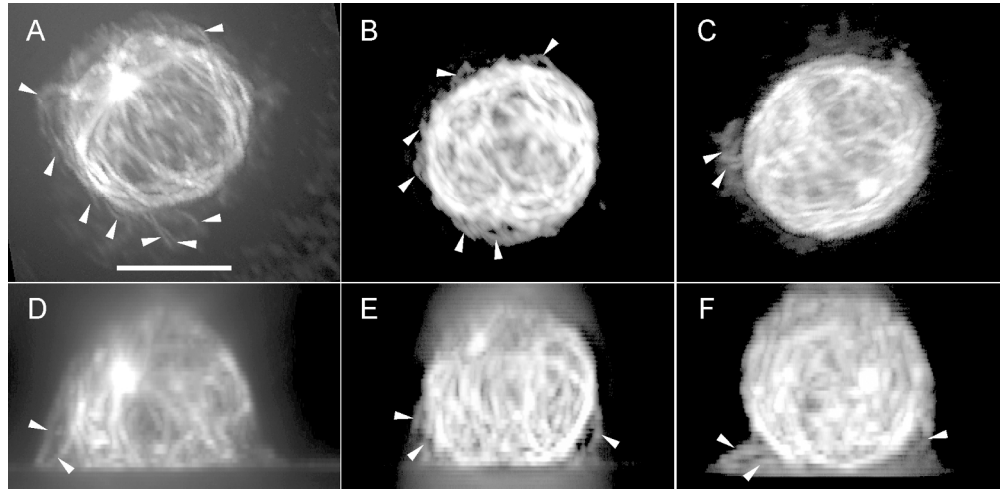


Fig. 5. Microtubules in Jurkat T lymphocytes. (A, B, C) Top views of three-dimensional immunofluorescence images of three cells. (D, E, F) Side views of the same three-dimensional images as in panels A, B, and C, respectively. Arrowheads indicate microtubules that appear to extend beyond the main body of the cell. Unsharp-masking has been employed for contrast enhancement. Scale bar, 10 μm .
172x83mm (300 x 300 DPI)

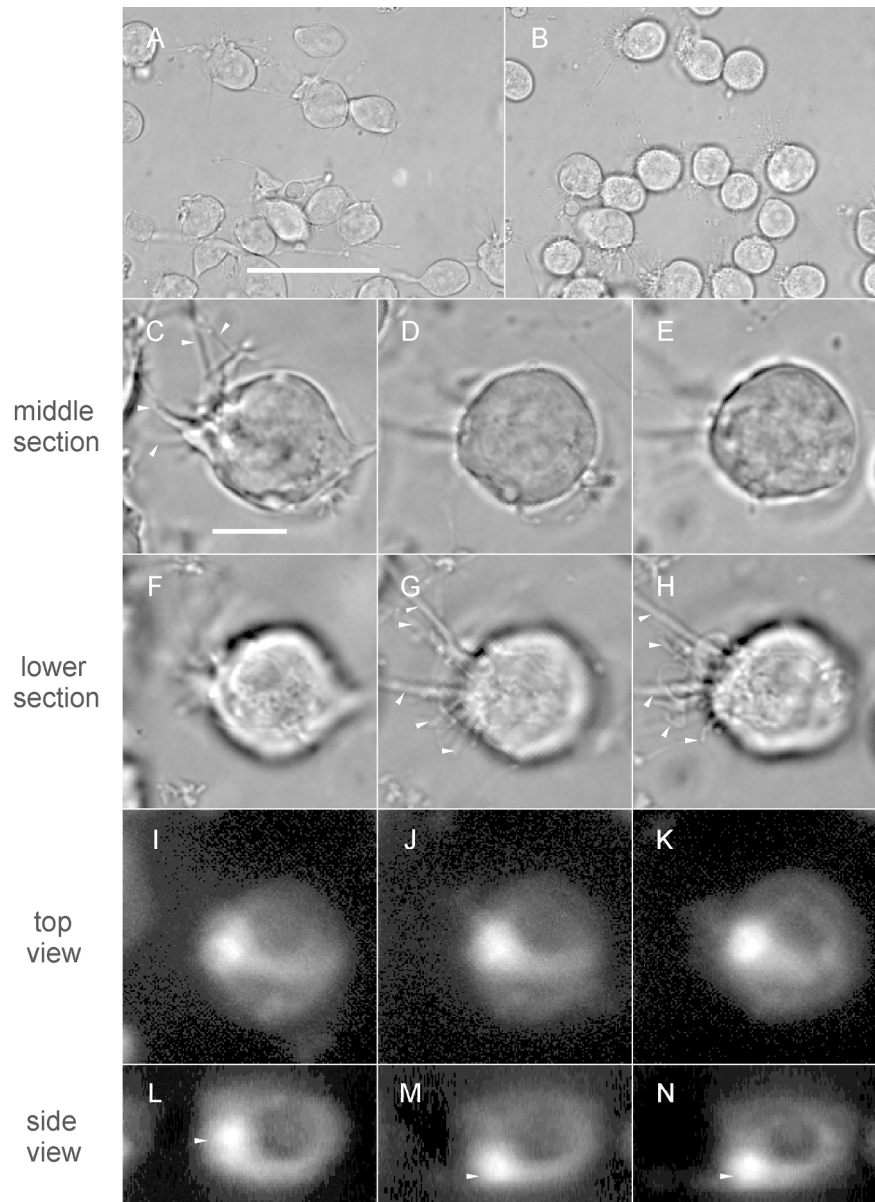


Fig. 6. Morphology, attachment, and polarization of cytochalasin-treated Jurkat T lymphocytes on an anti-TCR substrate. (A) 2 min after the cell suspension was introduced into the chamber and came in contact with the substrate. Scale bar, 50 μm . (B) The same field as shown in A, 20 min after introduction of the cell suspension. (C-N) Three-dimensional time-lapse images of a representative cell. Images in the first column (C, F, I, L), in the second column (D, G, J, M), and in the third column (E, H, K, N) were taken respectively in 2, 10, and 20 min after the introduction of the cell suspension. As labeled in the figure, two optical sections imaged in transmitted light are shown, as well as the top and side views of the full three-dimensional fluorescence image. The ceramide-based fluorescent probe in I-N reveals the plasma membrane and the Golgi apparatus area. Arrowheads in C, G, and H indicate the narrow tubulopodia. Arrowheads in L-N indicate the Golgi apparatus. The scale bar in C is 10 μm . Panels C-N refer to the same three-dimensional domain and have the same scale.

156x214mm (300 x 300 DPI)

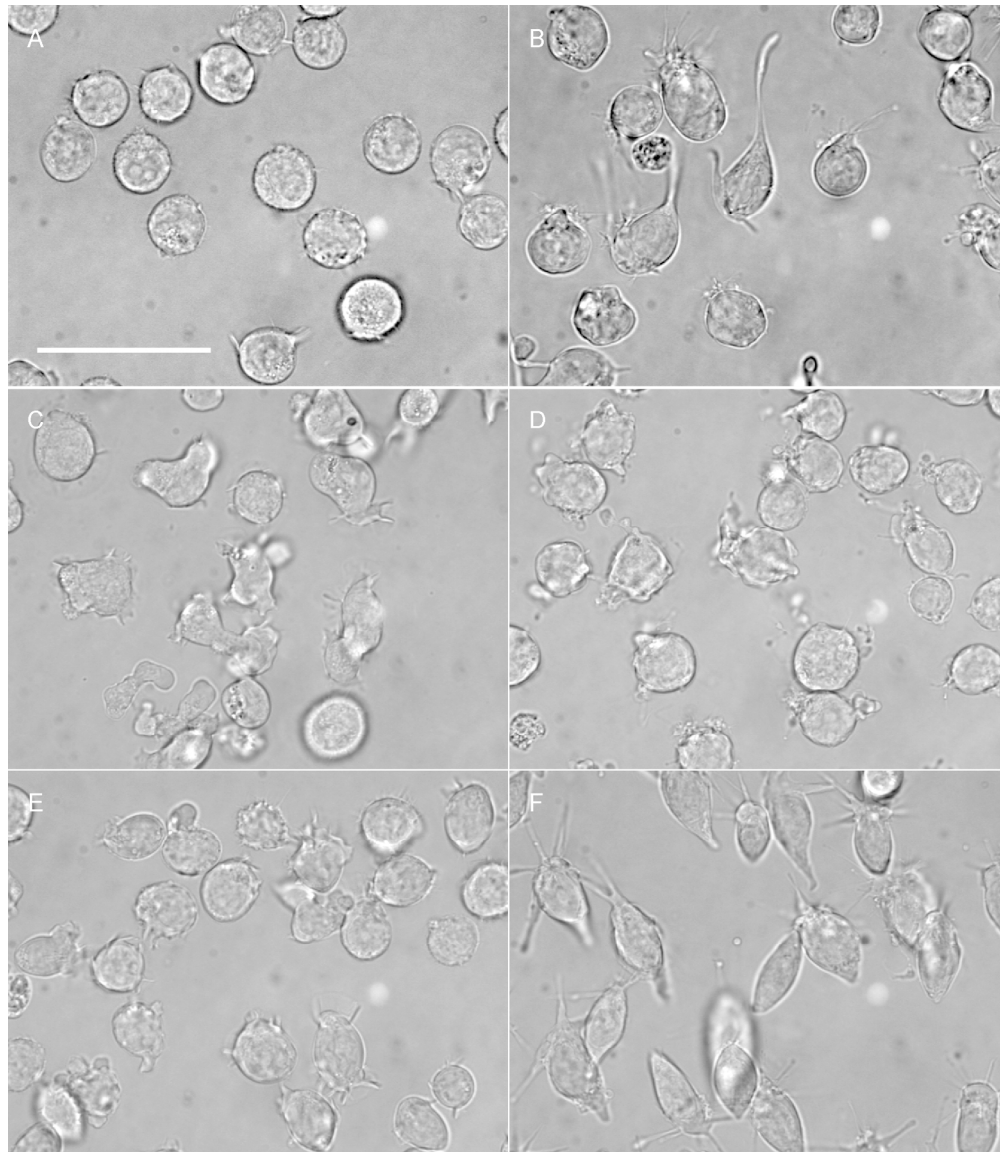


Fig. 7. Morphology of Jurkat T lymphocytes. (A) Cells treated with solvent only. (B) Cells treated with cytochalasin D. (C) Cells treated with nocodazole. (D) Cells treated with cytochalasin D and nocodazole. (E) Cells treated with paclitaxel. (F) Cells treated with cytochalasin D and paclitaxel. Scale bar, 50 μm .
170x195mm (300 x 300 DPI)

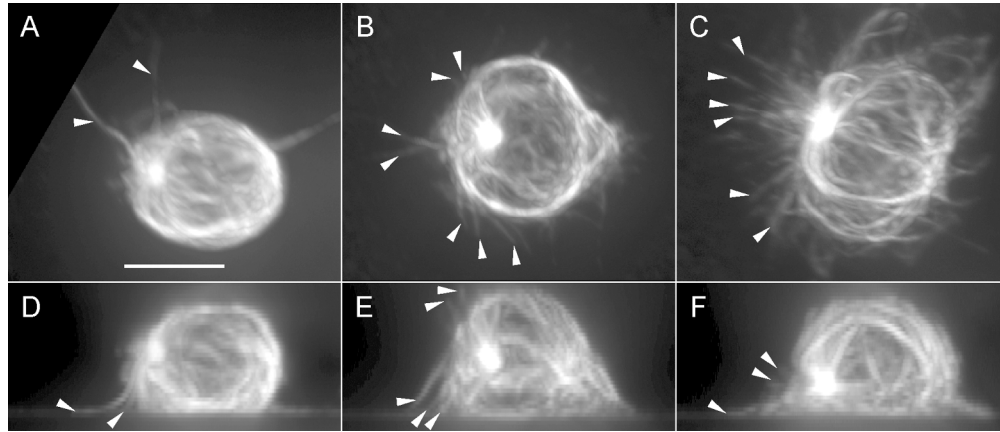


Fig. 8. Microtubules in Jurkat T lymphocytes treated with cytochalasin D. (A, B, C) Top views of three-dimensional immunofluorescence images of three cells. (D, E, F) Side views of the same three-dimensional images as in panels A, B, and C, respectively. Arrowheads indicate microtubules that appear to extend beyond the main body of the cell. Scale bar, 10 μm .
172x73mm (300 x 300 DPI)

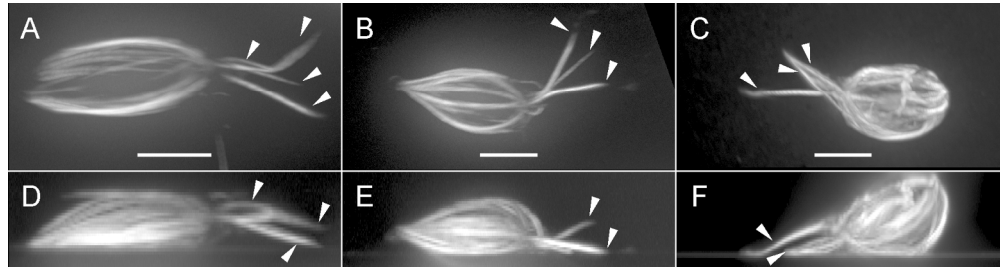


Fig. 9. Microtubules in Jurkat T lymphocytes treated with cytochalasin D and paclitaxel. (A, B, C) Top views of three-dimensional immunofluorescence images of three cells. (D, E, F) Side views of the same three-dimensional images as in panels A, B, and C, respectively. Arrowheads indicate microtubules or microtubule bundles that appear to extend beyond the main body of the cell. Scale bars, 10 μm .
170x44mm (300 x 300 DPI)

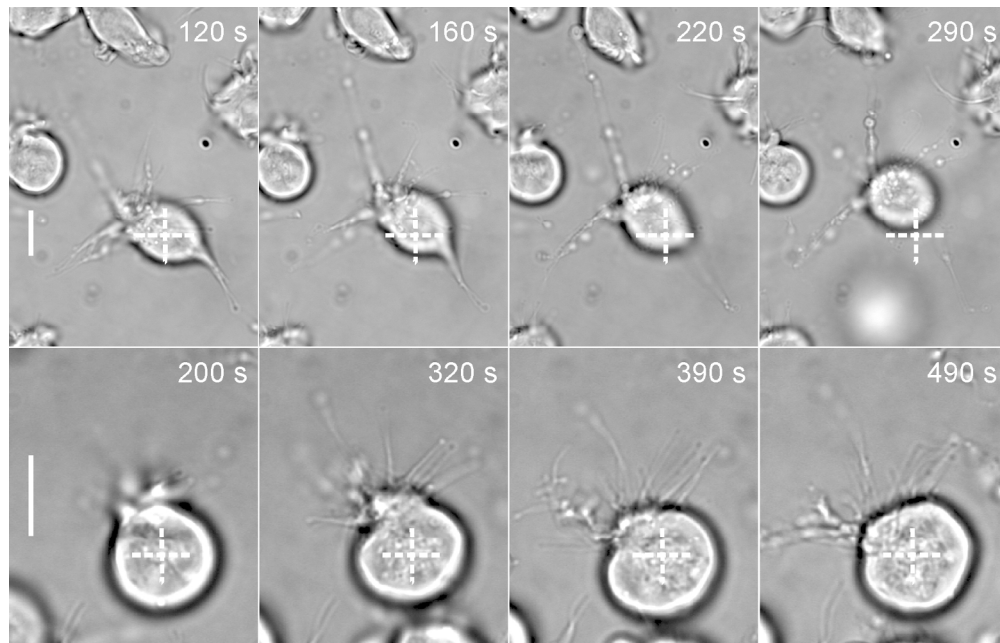


Fig. 10. Movement of Jurkat T lymphocytes treated with cytochalasin D on the anti-CD3-coated substrate. The top and bottom rows show time-lapse sequences of images of two different cells. Optical sections close to the substrate are shown. In each of the two image sequences, the cross marks a reference point that is fixed in the laboratory coordinates. The time indicated is the time elapsed after the cell suspension was brought in contact with the substrate. Scale bars, 10 μm . Note the tubulopodia gradually coming to focus, and the visual disappearance of the prominence where they emanate from the cell body. Both of these gradual visual changes are indicative of cell body rotation, and of reorientation of the tubulopodia emanation area to the substrate.

172x110mm (300 x 300 DPI)

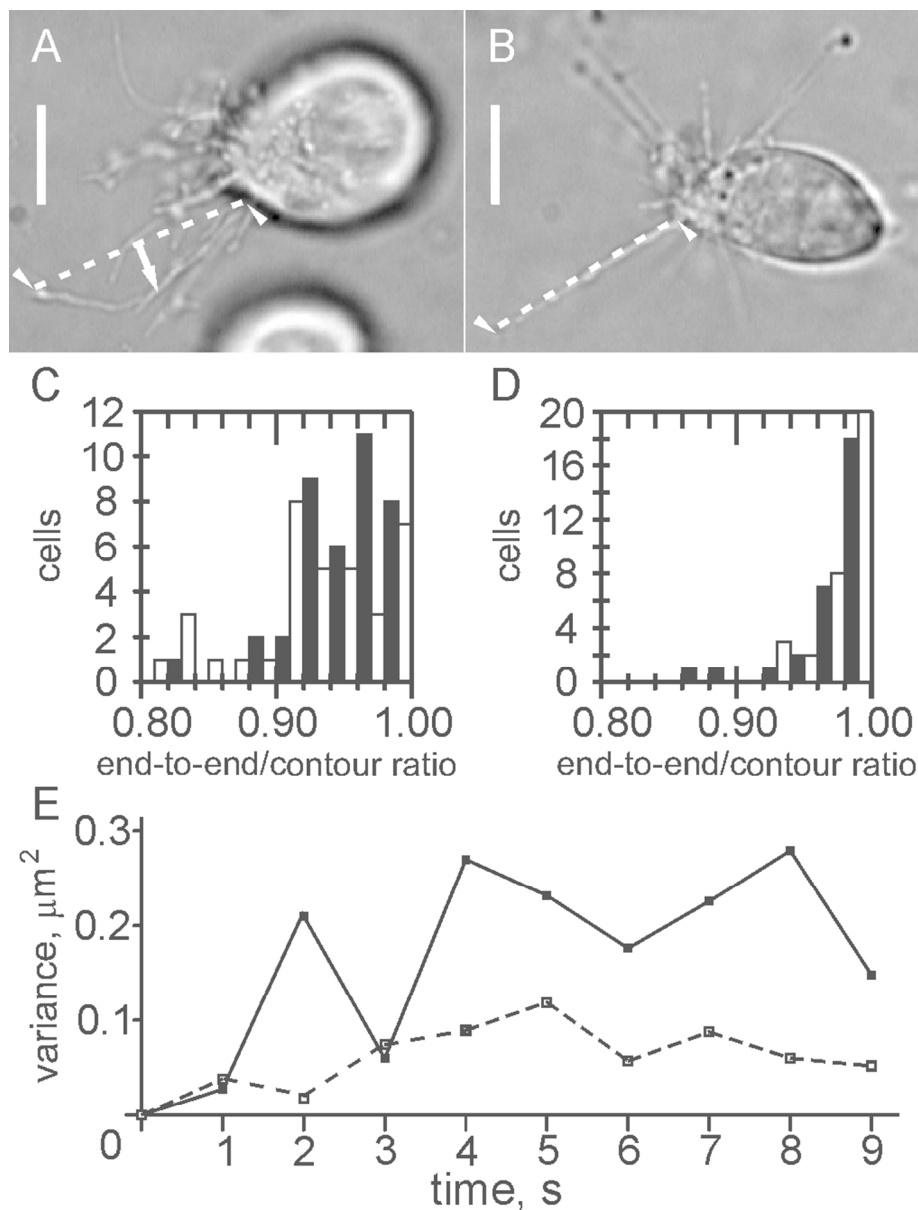


Fig. 11. Paclitaxel increases rigidity of tubulopodia. (A) A representative cell treated with cytochalasin D. (B) A representative cell treated with cytochalasin D and paclitaxel. Scale bars, 10 μm . Arrowheads indicate the two ends of the selected tubulopodia, which are also connected by the reference straight lines. In A, the arrow indicates the bend of the selected tubulopodium, defined as the deviation of the tubulopodium midpoint from the end-to-end straight line. (C, D) Histograms showing the distributions of the ratio of the end-to-end distance to the contour length of tubulopodia in cells treated with cytochalasin alone (C) and with cytochalasin and paclitaxel (D). Black bars represent measurements made in 150 s after the cell suspension was brought in contact with the anti-CD3-coated substrate. White bars represent measurements made in 600 s. One tubulopodium per cell was measured that was fully visible in the focal plane but otherwise selected randomly, and the data were pooled from 4 independent experiments. (E) Variance of the tubulopodia bend (defined in A) as a function of time. Solid line – cells treated with cytochalasin only. Dashed line – cells treated with cytochalasin and paclitaxel. In each experimental group, 8 tubulopodia were measured in 3 independent experiments. For each tubulopodium, the bend it displayed in the beginning of

the observation was taken for zero. Thus, the variance curves presented show the rapidity and extent of randomization of the tubulopodia bend with time.
85x112mm (300 x 300 DPI)

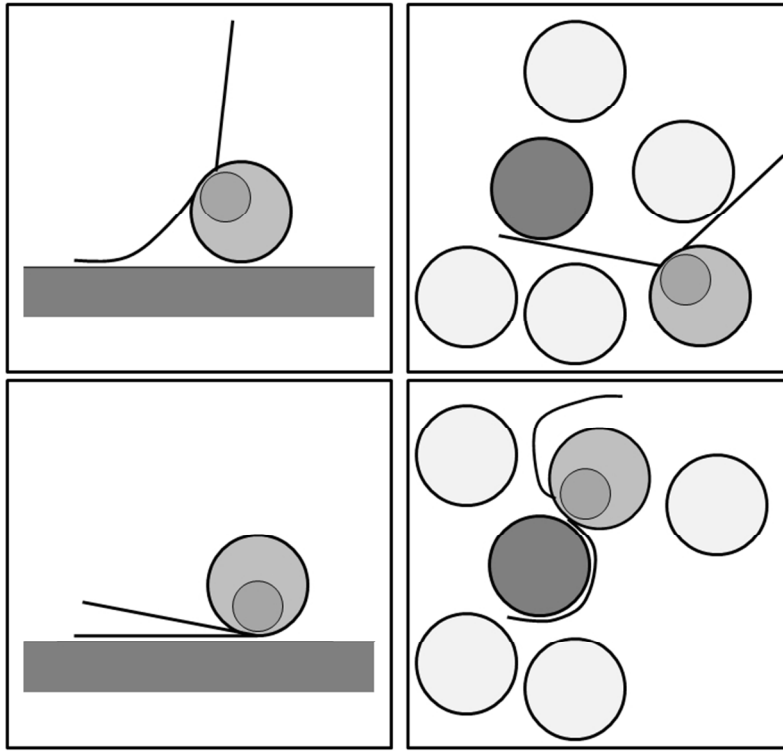


Fig. 12. Diagrammatic representation of cell motility mediated by tubulopodia. (A, B) Tubulopodia attachment and reorientation of the T-lymphocyte body to the TCR-binding substrate in the experimental model employed in the present work. (C, D) Hypothesized motility of a T lymphocyte with two tubulopodia in a dense tissue. Dark gray, the target cell. Light gray, bystander cells. The asymmetrical area containing the Golgi apparatus and the centrosome is shown inside the T lymphocyte.
254x190mm (96 x 96 DPI)